Abelian Manna model on two fractal lattices

Hoai Nguyen Huynh and Lock Yue Chew
Division of Physics and Applied Physics, School of Physical and Mathematical Sciences, Nanyang Technological University, Singapore, 21 Nanyang Link, Singapore 637371, Singapore

Gunnar Pruessner
Department of Mathematics, Imperial College London, 180 Queen's Gate, London SW7 2BZ, United Kingdom
(Received 28 June 2010; published 18 October 2010)

We analyze the avalanche size distribution of the Abelian Manna model on two different fractal lattices with the same dimension $d_g=\ln 3/\ln 2$, with the aim to probe for scaling behavior and to study the systematic dependence of the critical exponents on the dimension and structure of the lattices. We show that the scaling law $D(2-\tau)=d_w$ generalizes the corresponding scaling law on regular lattices, in particular hypercubes, where $d_w=2$. Furthermore, we observe that the lattice dimension d_g, the fractal dimension of the random walk on the lattice d_w, and the critical exponent D form a plane in three-dimensional parameter space, i.e., they obey the linear relationship $D=0.632(3)d_g+0.98(1)d_w-0.49(3)$.

DOI: 10.1103/PhysRevE.82.042103 PACS number(s): 05.70.Jk, 05.65.+b, 64.60.al

Although extensive research has been performed on self-organized criticality [1] for models on hypercubic lattices, far less work has been done on fractal lattices [2,3]. It remains somewhat unclear what to conclude from the latter studies. Fractal lattices are important for the understanding of critical phenomena for a number of reasons. First, results for critical exponents in lattices with noninteger dimensions might provide a means to determine the terms of their $\epsilon=4-d$ expansion. Second, fractal lattices are particularly suitable for real-space renormalization-group procedures, in particular those by Migdal [4], Kadanoff [5], and Carmona *et al.* [6]. Third, scaling relations that are derived in a straightforward fashion on hypercubic lattices can be put to test in a more general setting. In this Brief Report, we address the first and the third aspects by examining both numerically and analytically the scaling behavior of the Abelian version of the Manna model [7–9] on two different fractal lattices.

The fractal lattices used in this study are generated from the arc-fractal system [10]. The lattice sites are the invariant set of points of the arc-fractal. We consider nearest-neighbor interactions among sites. Here, the nearest neighbors of a given site are all sites which have the (same) shortest Euclidean distance to it. Our fractal lattices have no natural boundary; instead, they have only two end points at which two copies can join to form a bigger lattice. The dimension of the lattices is the same as the arc-fractal that generates them.

In this study, we shall consider two fractal lattices: the Sierpinski arrowhead and the crab (see Fig. 1). The former is named "Sierpinski arrowhead" because it is the same as the well-known Sierpinski arrowhead [11], whereas the latter is termed "crab" because the overall shape of the generated lattice looks like a crab. These fractal lattices are generated through the arc-fractal system with a number of segments $n=3$ and an opening angle of the arc $\alpha=\pi$. For the Sierpinski arrowhead, the rule for orientating the arc at each iteration is "in-out-in," while the rule is "out-in-out" for the crab. Both lattices have the same dimension $d_g=\ln 3/\ln 2\approx 1.58$. The total number of sites on the lattice at the ith iteration is $N_i=3^i+1$. The coordination number of sites on these lattices varies between two and three. Asymptotically, one third of the sites have three nearest neighbors (called extended sites), while the remaining two thirds have two nearest neighbors (called normal sites). Since the lattice sites are being stringed up by arcs (see Fig. 1), they can be labeled as sites on a one-dimensional (1D) linear chain. In order to determine the linear size (to be used in finite-size scaling) of the lattice, reference sites (hollow circles, which are not part of the lattice) have been added between the real sites (solid circles). This is possible because of the uniform spacing between sites. The linear size is then equal to the total number of hollow and solid circles along L (see Fig. 1). At the ith iteration, the linear size is given by $L_i=2^i+1$ for the arrowhead lattice and $L_i=3\times 2^{i-1}$ for the crab lattice. Indeed, one observes that the dimension of the lattice obeys the following

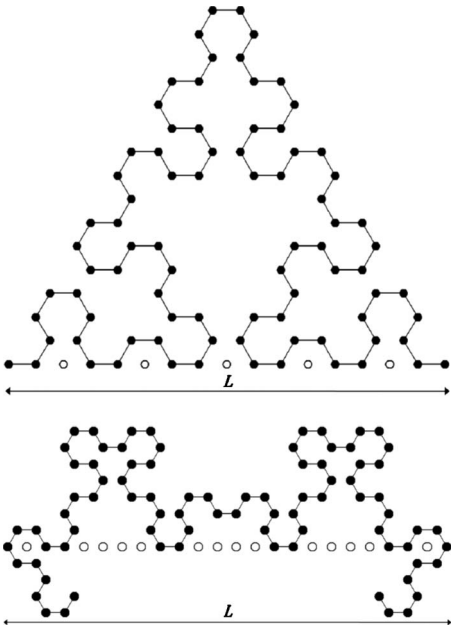

FIG. 1. Sierpinski arrowhead (top) and crab (bottom) lattices at fourth iteration with definition of linear size. In the figure, $L=17$ for arrowhead and $L=24$ for crab lattice.

relation with the total number of sites and linear size of the lattice: $d_g = \lim_{i\to\infty} \ln N_i / \ln L_i$.

We implement the Abelian Manna model on these two fractal lattices that have the same dimension but possess different microscopic structures. Let us denote the variable z_j, which is a non-negative integer, to be the "height" or the number of particles at lattice site j. The lattice is first initialized with $z_j=0$ for all sites. The value of z_j is then evolved according to the following algorithm. When the system is in a stable configuration, i.e., $z_j \leq 1$ for all sites, the external drive is implemented by picking a site j at random and increasing its z_j by 1 unit. At this juncture, an avalanche might occur in the following manner: as long as there exist any j with z_j exceeding the threshold $z_c=1$ (an "active" site), pick one of them at random, say k, and reduce z_k by 2. At the same time, pick two of its nearest neighbors, say k', randomly and independently, and increment $z_{k'}$ by 1 unit. This procedure constitutes a toppling, which in the bulk is conservative, i.e., the total $\Sigma_j z_j$ remains unchanged by the bulk topplings. In one dimension, every bulk site has two neighbors. On the fractal lattices described above, a bulk site can have either two or three nearest neighbors. Note that particles can leave the system at the two end sites (labeled as 1 and 3^i+1, respectively). Owing to the Abelianess of the model, the statistics of the avalanche sizes is independent of the order of updates. This is different for time-dependent observables such as the avalanche duration, which is not studied in the following.

An avalanche ceases as soon as $z_j \leq 1$ for all j (quiescence). The size s of the avalanche is measured as the number of topplings performed between two quiescent configurations. The probability density $\mathcal{P}(s)$ for an avalanche of size s to occur is expected to follow a simple (finite-size) scaling,

$$\mathcal{P}(s) = as^{-\tau}\mathcal{G}\left(\frac{s}{bL^D}\right), \tag{1}$$

asymptotically in large $s \gg s_0$ with lower cutoff s_0, linear system size L, nonuniversal metric factors a and b, and universal exponents τ and D. The universal scaling function $\mathcal{G}$ decays, for large arguments, faster than any power law, so that all moments $\langle s^q \rangle = \int ds \mathcal{P}(s) s^q$ exist for any finite system. Provided that $q+1-\tau > 0$ one can easily show that $\langle s^q \rangle \propto L^{D(q+1-\tau)}$.

The results presented in the following are based on Monte Carlo simulations for four different system sizes, corresponding to four different levels of iteration $i=3,4,5,6$, containing $N=28,82,244,730$ sites and with linear sizes $L=9,17,33,65$ for the Sierpinski arrowhead lattice and $L=12,24,48,96$ for the crab lattice. In all four cases, 10^8 avalanches were triggered and the data were recorded in regular intervals of 10^6 avalanches. Stationarity was verified by inspecting avalanche size moments, and the transient was determined to be shorter than 5×10^4 avalanches. Errors for the moments are derived from a jackknife estimator [12,13] of the variance based on the moments taken in each set of 10^6 measurements. The scaling exponents were determined by a nonlinear least-squares fitting [14] of the avalanche size moments against the linear size of the lattice:

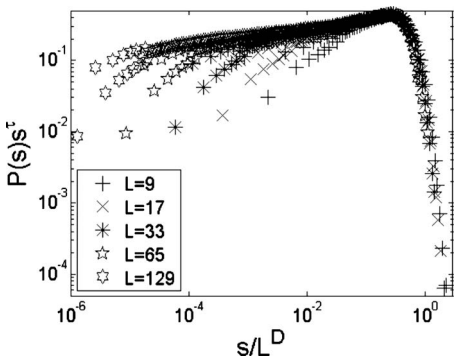

FIG. 2. Data collapse of binned data for Sierpinski arrowhead lattice. Preliminary statistics of large system size (seventh iteration, $L=129$) are also included to test the consistency of the data. The plots confirm the estimated values of the critical exponents.

$$\langle s^q \rangle = \left(a_q + \frac{b_q}{L} + \frac{c_q}{L^2}\right) L^{D(q+1-\tau)}. \tag{2}$$

The exponents derived in this procedure were $\tau=1.170(5)$ and $D=2.792(2)$ for the arrowhead lattice, and $\tau=1.153(4)$ and $D=3.026(2)$ for the crab lattice. In addition, the scaling behavior can be probed in a data collapse, as illustrated in Fig. 2.

With the critical exponents determined, one can immediately verify the scaling law of avalanche size distribution. From hypercubic lattices it is well known [15] that the first moment of the avalanche size is given by the expected number of moves that a random walker performs on the given lattice before it reaches the boundary and leaves, i.e., by its residence time. This is essentially because of bulk conservation: in the stationary state one particle leaves the system for every particle added (avalanche attempt), and the average number of moves it performs during its residency is exactly twice the average number of topplings occurring in the system per particle added, which is the avalanche size. Regardless of the specifics of the boundary, i.e., regardless of whether only two sites are dissipative or all sites along the perimeter, the first moment normally scales with the linear size of the lattices squared, $D(2-\tau)=2$, *independent of the dimension of the hypercubic lattice*. This is easily understood, as the time and thus the total number of moves performed by a random walker scale quadratically in the linear distance traversed.

For the fractal lattices, it is obvious that $D(2-\tau)$ is not equal to 2 since it is 2.317(8) for the arrowhead lattice and 2.564(6) for the crab lattice. We will now show that the scaling law has in fact changed to $D(2-\tau)=d_w$, where d_w is the fractal dimension of random walk on the lattice. The scale law $D(2-\tau)=d_w$ remains true for any lattice regardless of dimension and microscopic details.

We will now calculate d_w for the Sierpinski arrowhead lattice and the crab lattice by using the first-passage time method [16]. Due to the nearest-neighbor structure of the fractal lattices, the calculation is *not* coarse-grained renormalizationlike, but rather, it is carried out by considering every single edge that connects between the two end sites on the lattice.

TABLE I. Convergence of $S^{(i)}_{(3^i+1)/2}$ (first row of the pair) and $S^{(i)}_{(3^{i-1}+3)/2}$ (second row of the pair) as the number of iterations i increases. After $i=7$, we have $S^{(i)}_{j(i)} \approx 5$ for the Sierpinski arrowhead lattice and $S^{(i)}_{j(i)} \approx 6$ for the crab lattice. $S^{(i)}_{j(i)}$ for site near the end sites is also found to converge to the same limits but with slower convergence rate.

i	1	2	3	4	5	6	7
Arrowhead	5.5	4.6414	4.3821	4.6129	4.7808	4.8949	4.9768
	4.5	3.9815	4.1819	4.4213	4.6528	4.8163	4.9293
Crab	5.0	5.7611	6.2783	6.0906	5.9709	5.9655	5.9406
	4.0	6.2500	5.6300	6.0690	5.9934	5.9034	5.9355

We label the sites of the lattice sequentially with $j=1,2,\ldots,3^i+1$ and denote by $T^{(i)}_j$ the average time for the random walker to exit through the end sites from site j (i is the number of iterations of the lattice). Also, we denote by t the traverse time from one site to its nearest neighbor.

Let us define $E^{(i)}$ to be the set of extended sites at the ith iteration. On the lattice, each normal site j has two nearest neighbors $j-1$ and $j+1$. If j is an extended site, it has in addition a third nearest neighbor j^*. If the walker is at site j, we have two situations:

If $j \notin E^{(i)}$, the walker has only two options to choose from: go to $j-1$ or go to $j+1$. The probability for each choice is 1/2. We have

$$T^{(i)}_j = \tfrac{1}{2}(t + T^{(i)}_{j-1}) + \tfrac{1}{2}(t + T^{(i)}_{j+1}) = t + \tfrac{1}{2}T^{(i)}_{j-1} + \tfrac{1}{2}T^{(i)}_{j+1}. \quad (3)$$

Note that $T^{(i)}_0 = T^{(i)}_{3^i+2} = 0$.

If $j \in E^{(i)}$, the walker has up to three options to choose from: go to $j-1$, go to $j+1$, or go to j^*. The probability for each choice is 1/3. Thus, we have

$$T^{(i)}_j = \tfrac{1}{3}(t + T^{(i)}_{j-1}) + \tfrac{1}{3}(t + T^{(i)}_{j+1}) + \tfrac{1}{3}(t + T^{(i)}_{j^*}) = t + \tfrac{1}{3}T^{(i)}_{j-1} + \tfrac{1}{3}T^{(i)}_{j+1} + \tfrac{1}{3}T^{(i)}_{j^*}. \quad (4)$$

Since this gives a system of linear equations, we can write them in the form of a matrix equation: $A^{(i)}T^{(i)} = B^{(i)}$, where $T^{(i)}$ is the column vector of $T^{(i)}_j$, $A^{(i)}$ is the degree-normalized adjacency matrix, while $B^{(i)}$ is a column vector that contains t in every entry. As $A^{(i)}$ is invertible, we can solve for $T^{(i)} = (A^{(i)})^{-1}B^{(i)}$. By defining the variable $S^{(i)}_{j(i)} = T^{(i+1)}_{j(i+1)}/T^{(i)}_{j(i)}$, where site $j(i)$ at the ith iteration refers to a specific relative position on the lattice [for example, position of the site on top of the lattice $j(i)=(3^i+1)/2$ or the site connecting the lattice at the bottom $j(i)=(3^{i-1}+3)/2$], we obtain the results as shown in Table I and Fig. 3 for the arrowhead lattice and the crab lattice.

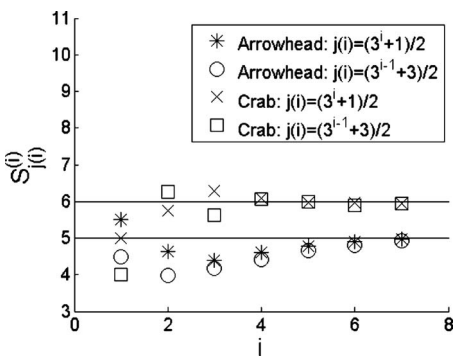

FIG. 3. Convergence of $S^{(i)}_{(3^i+1)/2}$ and $S^{(i)}_{(3^{i-1}+3)/2}$ as the number of iterations i increases. After $i=7$ we have $S^{(i)}_{j(i)}=5$ for arrowhead lattice and $S^{(i)}_{j(i)} \approx 6$ for crab lattice. $S^{(i)}_{j(i)}$ for site near the end sites is also found to converge to the same limits, but with slower convergence rate.

We observe that for both lattices $S^{(i)}_{j(i)}$ converges to some value $S^*_{j(i)}$ as i increases. For the arrowhead lattice, $S^*_{j(i)}=5$, while for the crab lattice, $S^*_{j(i)} \approx 6$. On going from the ith to $(i+1)$th iteration, the lattice size increases by a factor of $L_{i+1}/L_i = 2$, while the escape time increases by a factor of $T^{(i+1)}/T^{(i)} = S^*_{j(i)}$ for large i, so that $d_w = \ln S^*_{j(i)}/\ln 2$. By comparing the calculated d_w to the estimated value of $D(2-\tau)$ from simulation, we can see that they are in good agreement (see Table II).

One surprising conclusion from the above results is that for two lattices with the same dimension but different microscopic structures, the critical exponents D and τ can both be different, which suggests that on fractal lattices, the critical exponents depend not only on the dimension but also on the microscopic details of the lattice. In addition, our results have validated the scaling relation $D(2-\tau)=d_w$ for two fractal lattices with different d_w's. Since on lattices with integer dimensions $d_w=2$ regardless of the lattice's structure, this scaling relation generalizes the standard version $D(2-\tau)=2$ known for the hypercubic lattices. The last unexpected conclusion pertains to the relation between the dimensions d_g and d_w, and the critical exponent D. We found that they obey the general linear relationship $D=\alpha d_g+\beta d_w+\gamma$. This was uncovered by plotting the following six points in three-dimensional (3D) parameter space: $(d_g,d_w,D)=(1,2,2.1)$, $(2,2,2.73)$, $(3,2,3.36)$, $(4,2,4)$, $(1.58,2.32,2.79)$, $(1.58,2.58,3.03)$, which correspond to the linear chain [15], the square [7,17], the cube [18,19], the hypercube [20], the arrowhead, and the crab lattices, respectively. It is interesting that while the first four points due to the hypercubic

TABLE II. The calculated d_w and the estimated $D(2-\tau)$ for the Sierpinski arrowhead lattice and the crab lattice.

Lattice	Arrowhead	Crab
d_w	2.322	2.578
$D(2-\tau)$	2.317 ± 0.008	2.564 ± 0.006

TABLE III. Data for (d_g, d_w, D) from six different lattices and the calculated D_{trial} from Eq. (5).

Lattice	1D	2D	3D	4D	Arrowhead	Crab
d_g	1	2	3	4	1.58	1.58
d_w	2	2	2	2	2.32	2.58
D	2.2(1)	2.73(2)	3.36(1)	4	2.792(2)	3.026(2)
D_{trial}	2.10(7)	2.73(7)	3.36(7)	4.00(7)	2.78(7)	3.03(7)

lattices are found to lie on a straight line, all six points together make up a plane instead of a tetrahedron. We have determined the coefficients $\alpha = 0.632 \pm 0.003$, $\beta = 0.980 \pm 0.014$, and $\gamma = -0.492 \pm 0.034$ from the six points, which leads to the following relationship:

$$D \approx D_{trial}(d_g, d_w) = 0.632 d_g + 0.980 d_w - 0.492. \quad (5)$$

A comparison of the value of D determined by Eq. (5) and that from the simulation is shown in Table III.

Finally, we comment on the slight mismatches between the calculated d_w and the estimated $D(2-\tau)$ in Table II. They seem to be caused by finite-size corrections, which are further suppressed at seven iterations and above, as observed in preliminary data not included in the main analysis above. In the presence of strong finite-size corrections and high-accuracy measurements of the moments, the estimates for D and τ are sensitive to the choice of the fitting function, which is constrained by the number of data points (i.e., system sizes) available, but needs to contain as many correction terms as possible to account for the accurate data. Our choice (2) reflects the desire to reduce the sensitivity of the estimate on the initial values.

It is important to note that there is a level of ambiguity in the finite-size scaling in fractal lattices, because due to its highly irregular nature, there is *a priori* no unique way of increasing the lattice size of a fractal [21]. At a given level of iterations, in order to increase the lattice size further, one might either proceed by iterating the fractal or use the given fractal to tessellate the hypercubic lattice of appropriate (embedding) dimension. One might argue that finite-size scaling is of course sensitive to that choice and, as a result, generates *asymptotically* the exponents either of the fractal lattice or of the embedding space. However, in ordinary critical phenomena, there are cases [21] where the (effective) critical point and even the scaling functions change with the level of iteration i. In the current context that translates to, for example, the amplitude $A_q = a_q + b_q/L + c_q/L^2$ in Eq. (2) to acquire a dependence on i, which might distort the resulting estimates. The exponents derived above can thus be seen only as *effective* exponents of a fractal lattice.

[1] P. Bak, C. Tang, and K. Wiesenfeld, Phys. Rev. Lett. **59**, 381 (1987).
[2] B. Kutnjak-Urbanc, S. Zapperi, S. Milosevic, and H. E. Stanley, Phys. Rev. E **54**, 272 (1996).
[3] K. E. Lee, J. Y. Sung, M. Y. Cha, S. E. Maeng, Y. S. Bang, and J. W. Lee, Phys. Lett. A **373**, 4260 (2009).
[4] A. A. Migdal, Sov. Phys. JETP **42**, 413 (1976).
[5] L. P. Kadanoff, Ann. Phys. (N.Y.) **100**, 359 (1976).
[6] J. M. Carmona, U. M.B. Marconi, J. J. Ruiz-Lorenzo, and A. Tarancón, Phys. Rev. B **58**, 14387 (1998).
[7] S. S. Manna, J. Phys. A **24**, L363 (1991).
[8] D. Dhar, Physica A **263**, 4 (1999).
[9] D. Dhar, Physica A **369**, 29 (2006).
[10] H. N. Huynh and L. Y. Chew (unpublished), available at http://www.worldscinet.com/fractals/editorial/paper/910421.pdf
[11] B. B. Mandelbrot, *The Fractal Geometry of Nature* (W. H. Freeman, New York, 1982), pp. 141–142.
[12] B. Efron, *The Jackknife, the Bootstrap and Other Resampling Plans* (SIAM, Philadelphia, PA, 1982).
[13] B. A. Berg, Comput. Phys. Commun. **69**, 7 (1992).
[14] W. H. Press, S. A. Teukolsky, W. T. Vetterling, and B. P. Flannery, *Numerical Recipes*, 3rd ed. (Cambridge University Press, Cambridge, UK, 2007).
[15] H. Nakanishi and K. Sneppen, Phys. Rev. E **55**, 4012 (1997).
[16] D. ben-Avraham and S. Havlin, *Diffusion and Reactions in Fractals and Disordered Systems* (Cambridge University Press, Cambridge, UK, 2000), pp. 61–64.
[17] A. Chessa, H. E. Stanley, A. Vespignani, and S. Zapperi, Phys. Rev. E **59**, R12 (1999).
[18] R. Pastor-Satorras and A. Vespignani, Eur. Phys. J. B **19**, 583 (2001).
[19] A. Ben-Hur and O. Biham, Phys. Rev. E **53**, R1317 (1996).
[20] S. Lübeck, Int. J. Mod. Phys. B **18**, 3977 (2004).
[21] G. Pruessner, D. Loison, and K.-D. Schotte, Phys. Rev. B **64**, 134414 (2001).